Shock-induced anisotropy of magnetic susceptibility: impact experiment on basaltic andesite

Itoyuki Nishioka[1], Minoru Funaki[2], and Toshimori Sekine[3]

[1]*The Graduate University for Advanced Studies, Hayama, Kanagawa 240-0193, Japan*
[2]*National Institute of Polar Research, Itabashi, Tokyo 173-8515, Japan*
[3]*National Institute for Materials Science, Tsukuba, Ibaraki 305-0044, Japan*

(Received August 27, 2007; Revised October 3, 2007; Accepted October 9, 2007; Online published October 30, 2007)

Changes in the anisotropy of the low-field magnetic susceptibility (AMS) of basaltic andesite were induced by decaying stress waves and subsequently quantified. An initial shock pressure of 5 GPa was generated in a block of the target rock through impacting with a cylindrical projectile. Following the impact, the maximum or minimum principal susceptibility axes of the target were reoriented toward the shock direction at low (0.5–3 GPa) or high (>3 GPa) estimated shock pressures, respectively. Subtraction of the initial AMS demonstrated a parallelism between the induced susceptibility axes and the shock direction. These results suggest a potential application of AMS as an indicator of the propagation directions of stress waves generated in rocks at terrestrial impact structures.

Key words: Anisotropy of magnetic susceptibility, magnetic hardening, stress waves, basaltic andesite, impact crater.

1. Introduction

The effects of high pressures on rock magnetic properties are of interest in terms of gaining an understanding of the magnetism of rocks subjected to strong stress waves, such as lunar rocks and meteorites (paleomagnetic records) and terrestrial planets and satellites (crustal magnetization). The results of laboratory shock experiments reveal that the primary effects of impact are demagnetization or remagnetization, and magnetic hardening (Gattacceca *et al*., 2007 and references therein). Gattacceca *et al*. (2007) also demonstrated that explosive-driven shocks of about 10 GPa on basalt and microdiorite acted to change the anisotropy of their low-field magnetic susceptibility (AMS). The AMS of terrestrial rock is usually controlled by the preferred orientation of the magnetic minerals related to the primary formation of the rock or its subsequent tectonic deformation. An important implication of the results of the above-mentioned shock experiments is that the minimum principal susceptibility axes are reoriented toward the shock directions, indicating that AMS may be a proxy to the propagation direction of ancient stress waves in rocks.

We have conducted a laboratory impact experiment aimed at studying the shock-induced changes in AMS parameters in detail. We describe here the observed changes in the shape, degree, and direction of AMS ellipsoids following an impact. To constrain the mechanism of these changes, we evaluated their stabilities against tumbling alternating field demagnetization (AFD) and changes in hysteresis parameters.

2. Experiments

Stress waves were produced in the rock target using a single-stage propellant gun (30-mm bore) housed at the National Institute for Materials Science, Japan. The target was a cubic block of basaltic andesite ($17 \times 17 \times 17$ cm) housed in a stainless steel (SUS 304) container. A cylindrical aluminum projectile with a diameter of 11.75 mm and length of 38 mm (weight: 46.0 g) was set on a high-density polyethylene sabot. The projectile was accelerated to an impact velocity of 0.725 ± 0.25 km/s to produce an initial pressure of 5.2 ± 0.2 GPa, as determined using the impedance match method. We used the Hugoniot data for aluminum reported in Marsh (1980) and that for basalt reported in Nakazawa *et al*. (1997). The duration of such a compression is considered to be in the order of microseconds (Nakazawa *et al*., 2002). The projectile impacted near the center of the target surface. The target remained intact except for the formation of a shallow surface crater (3 cm in diameter and 2 mm in depth). We observed many tensile cracks parallel to the impacted surface in the regions between the crater floor and a depth of 3 mm. Subvertical cracks and local fractures were observed at deeper levels within the target.

We then prepared 14 continuous cubic specimens ($6 \times 6 \times 6$ mm) from directly beneath the center of the crater floor, i.e. extending downwards to a depth of about 10 cm. The specimens were numbered i01, i02, i03, etc., beginning with the uppermost specimen. Five control specimens of the same size—which we assumed to be less shocked than the specimens from the central area—were cut off from the side of the target block (at 8 cm distance from the crater center, in the region near the impact surface). Pressure decay beneath the impact point was estimated after Nakazawa *et al*. (2002), whose planar shock experiments on basalts revealed that the relationship between the mea-

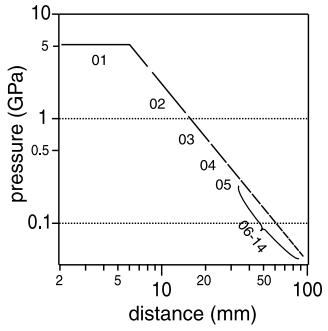

Fig. 1. Pressure decay beneath the impact point (see text for equations).

Table 1. Magnetic hysteresis parameters of basaltic andesite from Mt. Omuro at room temperature.

H_c (mT)	H_{cr} (mT)	I_s (A m^2/kg)	I_r (A m^2/kg)	K_p (m^3/kg)
9.5	21.0	0.50	0.12	2.29E-07

Notes: Coercivity, H_c; remanence coercivity, H_{cr}; saturation magnetization, I_s; saturation remanence, I_r; and high-field magnetic susceptibility, K_p.

sured shock pressure, P, and the distance beneath the impact surface, x, can be formulated as $P/P_0 = 1(x \leq r)$, $P/P_0 = (x/r)^{-1.7}(x > r)$, where P_0 is the initial pressure and r is the projectile radius. These equations were used in the present study to obtain estimates of the pressure ranges for each specimen (Fig. 1).

Low-field magnetic susceptibility and its anisotropy (AMS) were measured at room temperature (25°C) using an AGICO KLY-3S Kappabridge. The operating frequency and field intensity were 875 Hz and 0.4 mT, respectively. AMS was measured before and after two-axis tumbling AFDs in a peak field of 80 mT. The average low-field susceptibility, K_m, was calculated as $K_m = (K_1 + K_2 + K_3)/3$, where K_1, K_2, and K_3 are the principal susceptibilities ($K_1 \geq K_2 \geq K_3$). The shapes of the AMS ellipsoids were characterized in terms of a shape parameter, T, and anisotropy degrees, P' after Jelinek (1981). We also measured hysteresis curves of the same specimens at room temperature with a maximum field of 1.0 T and using a vibrating sample magnetometer (Riken Denshi, BHV-50). The average hysteresis parameter for each specimen was calculated as $(A_p + 2 \times A_n)/3$, where A_p and A_n are the hysteresis parameters measured parallel and perpendicular to the shock direction, respectively.

3. Initial Mineralogy and Magnetic Properties

The target rock was sampled from Quaternary lava flows at Mt. Omuro, Izu Peninsula, Central Japan. The bulk density of the basaltic andesite, as measured from a cylindrical core, was 2.74 g/cm^3. This value is similar to those recorded for basalts (2.63–2.74 g/cm^3) used in previous shock attenuation experiments (Nakazawa *et al.*, 2002). The petrology and mineralogy of the target rock is described in Hamuro (1985). The sample contains phenocrysts of olivine and plagioclase in a groundmass of plagioclase, augite, hypersthene, pigeonite, and titanomagnetite.

A reversible thermomagnetic curve in a vacuum ($\sim 10^{-3}$ Pa) was obtained up to 600°C using the vibrating sample magnetometer. A single Curie point at 180°C in-

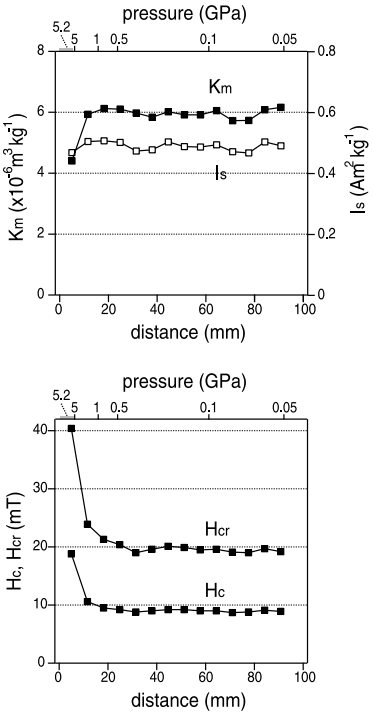

Fig. 2. Post-impact magnetic parameters of the target rock as a function of the distance from the impacted surface toward the center of the specimen. Low-field magnetic susceptibility, K_m; saturation magnetization, I_s; coercivity, H_c; remanence coercivity, H_{cr}.

dicates the presence of $Fe_{2.4}Ti_{0.6}O_4$ or TM60 (Akimoto *et al.*, 1957). Magnetic hysteresis parameters at room temperature after slope correction are shown in Table 1. The titanomagnetite content was estimated to be 1.1 vol.% based on a saturation magnetization (I_s) of 125 kA/m expected for stoichiometric TM60 (Dunlop and Özdemir, 1997). A comparison of obtained M_s/M_r and H_{cr}/H_c values with data presented by Day *et al.* (1977) indicates that the present values correspond to a grain size of 3–6 μm of crushed TM60. Under the optical microscope, the titanomagnetite grains were observed to be 20 μm or smaller. The average ferromagnetic contribution to low-field susceptibility was determined to be 96%, as calculated using the average values of high-field susceptibility (K_p) and average low-field susceptibility (K_m).

4. Shock Effects on Hysteresis Parameters and AMS

The target between the depths of 10 and 100 mm showed no systematic change in K_m (Fig. 2, upper); the average value (±standard deviation) was $5.97 \pm 0.14 \times 10^{-6}$ m^3/kg, which is similar to the values obtained for the side specimens (data not shown; $5.95 \pm 0.11 \times 10^{-6}$ m^3/kg). Relative to areas in the lower part of the specimen, K_m was reduced by about 30% in areas close to the impact (i01); in contrast, saturation magnetization, I_s, was unaffected by the impact. The average I_s value of the beneath-crater specimens was 0.49 ± 0.02 A m^2/kg, which indicates the absence of any production of magnetic minerals via the shock decomposition of mafic minerals. The patterns of variations in K_m and I_s are similar among the lower specimens. Therefore, the K_m values of specimens i02–i14 did not show a significant

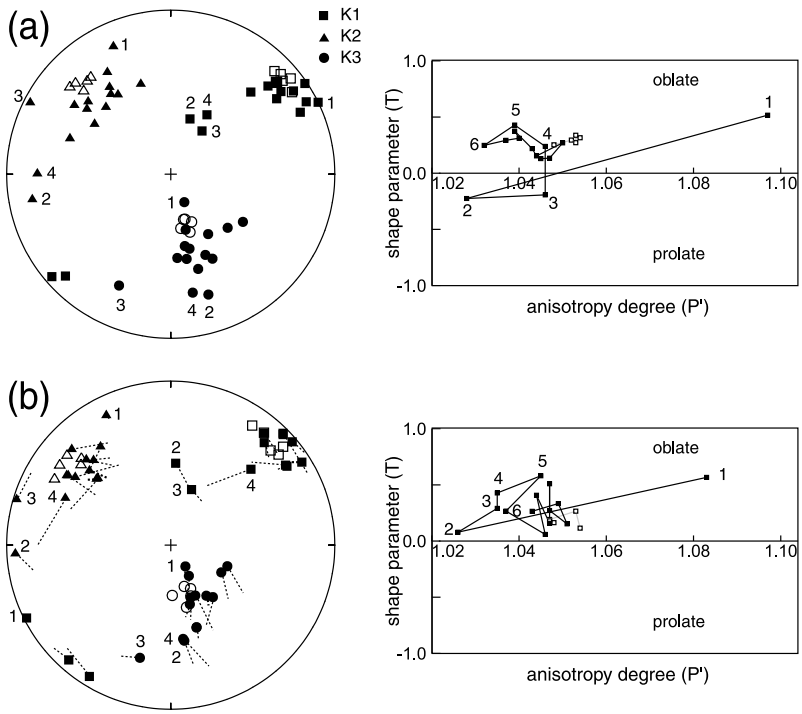

Fig. 3. AMS parameters of the target rock (a) before and (b) after tumbling AFD. The solid and open symbols denote data from specimens located beneath the impact point and from the side of the target block, respectively. Left: Lower hemisphere equal-area projection showing the orientations of the principal susceptibility axes. The vertical axis is the shock direction. Numbers denote specimen ID. The trajectories of the principal susceptibility axes before and after AFD are also shown. Right: plot showing the shape of the AMS ellipsoids. Anisotropy degree (P') and the shape parameter (T) are after Jelinek (1981).

decrease: the minor observed variations only reflect heterogeneity in the volume density of the magnetic grains. The decrease in K_m recorded for the uppermost specimen (i01) was associated with the impact. Coercivity, H_c, and the coercivity of remanence, H_{cr}, were generally constant for the lower specimens between i05 and i14, with average values of 9.0 and 19.5 mT, respectively (Fig. 2). These parameters increased by approximately 100% for specimen i01, and to a lesser extent for specimen i02 and, possibly, i03. The observed increase in coercivity and decrease in low-field susceptibility may be indicative of an increase in defect density (Jackson *et al.*, 1993). Coercivity is likely to provide a more sensitive measure of defect density than susceptibility (Heider *et al.*, 1996) because coercivity, unlike susceptibility, is related to irreversible magnetization processes; i.e., the pinning and unpinning of domain walls at lattice defects.

The orientations of the principal susceptibility axes are shown in Fig. 3(a) (left). Those of the side specimens show tightly clustered triaxial distributions, but the specimens from beneath the impact point show a wider distribution. For specimens from beneath the impact point, the inclinations of the minimum axes are generally shallower than those in the primary directions. The changes are most remarkable for specimens located close to the impact (i02–i04), for which the easy (K_1) axes are subparallel to the shock direction. In contrast, specimen i01 has the K_1 axis oriented close to the shock direction. Figure 3(a) (right) reveals that the AMS of the side and lower specimens shows slightly oblate ($T > 1$) AMS ellipsoids, with P' values of about 1.05. The side specimens record only minor variations in the AMS shape parameters. The AMS ellipsoids show a gradual change in shape with increasing pressure, with the shifts in the data points being more pronounced close to the impact point (i01–i05): specimen i01 records a high P' value. These results indicate that the observed changes in the shape, degree, and orientation of the AMS ellipsoids occur at a lower pressure than that leading to a reduction in K_m.

The principal susceptibility axes of the side specimens showed no significant change in orientation or shape of AMS ellipsoids following AFD (Fig. 3(b)); in contrast, the specimens sampled from directly beneath the impact showed a general change in their AMS parameters. The average orientations of the principal axes of the samples from directly beneath the impact changed to orientations similar to those of the side specimens. The lower specimens showed no significant changes in T and P' following AFD; however, remarkable shape changes were observed for specimens sampled from close to the impact.

5. Summary and Discussion

We classified the observed AMS changes into the following three levels: (1) low shock pressure of less than 0.5 GPa (specimens i05–i14) that induced only minor changes in the directions and shapes of the AMS ellipsoids; the shock effects were removed by tumbling AFD; (2) intermediate shock pressure ranging from 0.5 to 3 GPa (i02–i04) that produced K_1 axes oriented subparallel to the shock direction; tumbling AFD partly removes this effect; (3) high shock pressure of greater than 3 GPa (i01) that gave rise to a significant increase in P' and a decrease in K_m; the K_3 axis changed from the initial direction to the shock direction, and the new AMS was highly stable against AFD. Gattacceca *et al.* (2007) observed similar changes in AMS

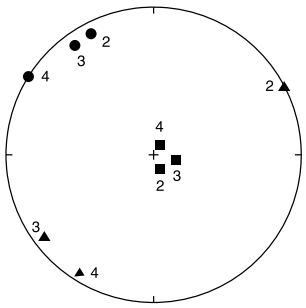

Fig. 4. A lower-hemisphere equal-area projection showing the orientations of the principal susceptibility axes for specimens i02–i04 before AFD and after the isolation of the shock-induced component. See Fig. 3 (left) for symbols.

for basalt and microdiorite shocked to pressure greater than 10 GPa.

The changes observed at low to intermediate shock pressures are generally similar to those reported from experiments involving static loading. Kapička (1988) reported that the elastic deformation of basalt arising from uniaxial stresses up to 60 MPa essentially caused reversible changes in AMS. This result indicates that the magnetic domains are ordered when subjected to the external stress but that they revert to the initial configuration with release of the stress (Appel and Soffel, 1985). However, small irreversible changes in AMS do occur (Kapička, 1983), probably related to the pinning of domain walls at lattice defects or the irreversible rotation of spontaneous magnetization to other easy axes. Such stress-induced anisotropy has been suggested to be removable by tumbling AF demagnetization (Park *et al.*, 1988). In contrast, the AMS changes recorded at intermediate to high shock pressures may be related to either the fracturing of magnetic grains (Gattacceca *et al.*, 2007) or the formation of lattice defects, such as dislocations. Both mechanisms are consistent with the high stability of the AMS changes against AFD (Fig. 3(b)). Optical microscopy confirmed that grain rotation is not responsible for the AMS changes.

The lack of an exact parallelism between the K_1 axes and the shock direction for the intermediate-pressure specimens can be explained by the effect of the primary AMS. We introduce a simple model in which the measured AMS (F_1) represents the superposition of primary (F_0) and shock-induced (F_s) AMS, each represented as second-rank symmetric tensors. In this case, F_s is easily determined by subtracting F_0 from F_1. We used the average tensor of the five-sided specimens as F_0. Figure 4 shows that specimens i02–i04 exhibit enhanced the parallelism of the K_1 axes after isolation of the shock components. At this time, we do not have a theoretical model to explain the K_1 axes oriented parallel to the shock direction. At higher pressures (specimen i01), the K_3 axis is oriented parallel to the shock (Fig. 3(a)); therefore, approximately 3 GPa of pressure is proposed as a threshold value at which a change occurs in the mechanism that governs the AMS of these specimens.

The parallelism of the induced low-field susceptibility and the shock axis highlights the potential use of AMS as an indicator of the propagation direction of stress waves. It is expected that the shock sensitivity of AMS is dependent on the composition and size of the magnetic minerals in the target rocks. Under the present experimental conditions, the observed AMS changes were induced under estimated pressures of as low as 0.5 GPa. The results of numerical modeling predict that this pressure range covers relatively large volumes of target rocks beneath impact craters (e.g., Ugalde *et al.*, 2005). Therefore, the application of AMS to known terrestrial impact structures would provide new insight into the process of impact-related cratering, while its application to suspected terrestrial impact structures would provide evidence of an impact origin. The results of our study also indicate that the resultant AMS is strongly affected by the relative orientation and degree of the primary AMS. The tensor subtraction (F_1–F_0) is virtually inapplicable for natural impact structures because no information is available on F_0, which is often variable, even within the same rock formation. The effects of weak shock may thus be less recognizable for rocks with a strong primary anisotropy.

Acknowledgments. We would like to thank Dr. Y. Syono for helpful discussion regarding this study. Drs. M. Jackson and J. Gattacceca provided useful suggestions that helped to improve the manuscript.

References

Akimoto, S., T. Katsura, and M. Yoshida, Magnetic properties of $TiFe_2O_4$-Fe_3O_4 system and their change with oxidation, *J. Geomag. Geoelectr.*, **9**, 165–178, 1957.

Appel, E. and H. C. Soffel, Domain state of Ti-rich titanomagnetites deduced from domain structure observations and susceptibility measurements, *J. Geophys.*, **56**, 121–132, 1985.

Day, R., M. Fuller, and V. A. Schmidt, Hysteresis properties of titanomagnetites: grain-size and compositional dependence, *Phys. Earth Planet. Inter.*, **13**, 260–267, 1977.

Dunlop, D. J. and Ö. Özdemir, *Rock Magnetism: Fundamentals and frontiers*, pp. 573, Cambridge University Press, Cambridge, 1997.

Gattacceca, J., A. Lamali, P. Rochette, M. Boustie, and L. Berthe, The effects of explosive-driven shocks on the natural remanent magnetization and the magnetic properties of rocks, *Phys. Earth Planet. Inter.*, **162**, 85–98, 2007.

Hamuro, K., Petrology of the Higashi-Izu monogenetic volcano group, *Bull. Earthq. Res. Inst. Univ. Tokyo*, **60**, 335–440, 1985.

Heider, F., A. Zitzelsberger, and K. Fabian, Magnetic susceptibility and remanent coercive force in grown magnetite crystals from 0.1 mm to 6 mm, *Phys. Earth Planet. Inter.*, **93**, 239–256, 1996.

Jackson, M., G. Borradaile, P. Hudleston, and S. Banerjee, Experimental deformation of synthetic magnetite-bearing calcite sandstones: effects on remanence, bulk magnetic properties, and magnetic anisotropy, *J. Geophys. Res.*, **98**(B1), 383–401, 1993.

Jelinek, V., Characterization of the magnetic fabric of rocks, *Tectonophysics*, **79**(3–4), 63–67, 1981.

Kapička, A., Irreversible changes of anisotropy of magnetic susceptibility of rocks due to uniaxial pressure, *J. Geophys.*, **53**(3), 144–148, 1983.

Kapička, A., Anisotropy of magnetic susceptibility in a weak magnetic field induced by stress, *Phys. Earth Planet. Inter.*, **51**(4), 349–354, 1988.

Marsh, S. P. (Ed.), *LASL Shock Hugoniot Data*, University of California Press, Berkeley, 1980.

Nakazawa, S., S. Watanabe, M. Kato, Y. Iijima, T. Kobayashi, and T. Sekine, Hugoniot equation of state of basalt, *Planet. Space Sci.*, **45**(11), 1489–1492, 1997.

Nakazawa, S., S. Watanabe, Y. Iijima, and M. Kato, Experimental Investigation of Shock Wave Attenuation in Basalt, *Icarus*, **156**, 539–550, 2002.

Park, J. K., E. I. Tanczyk, and A. Desbarats, Magnetic fabric and its significance in the 1400 Ma Mealy diabase dykes of Labrador, Canada, *J. Geophys. Res.*, **93**(B11), 13689–13704, 1988.

Ugalde, H. A., N. Artemieva, and B. Milkereit, Magnetization on impact structures—Constraints from numerical modeling and petrophysics, in *Large meteorite impacts III: Geological Society of America Special Paper 384*, edited by T. Kenkmann, F. Hörz, and A. Deutsch, pp. 25–42, 2005.

I. Nishioka (e-mail: nishioka@nipr.ac.jp), M. Funaki, and T. Sekine